

Buffon-Laplace Needle Problem with needles of arbitrary length

Jin-Hua Zhao*

School of Data Science and Engineering, South China Normal University, Shanwei 516622, China

(Dated: February 14, 2024)

Buffon-Laplace Needle Problem considers a needle of a length l randomly tossed on a large plane with vertically parallel lines with distances a and b ($b \leq a$), respectively. Previous results mainly focus on the ‘short needle’ case of $l \leq b$. Here we analytically calculate the probability of a needle of any l intersecting with lines, specifically in the cases of $l \leq b$, $b < l \leq a$, $a < l \leq \sqrt{a^2 + b^2}$, and $\sqrt{a^2 + b^2} < l$. Our theory naturally retrieves the analytical solution of Buffon’s Needle Problem when a goes to infinity. Our analytical framework is further confirmed by results from numerical simulation.

I. INTRODUCTION

Buffon’s Needle Problem [1] is the oldest problem in geometrical probability dated back more than two centuries. It considers randomly dropping a one-dimensional needle with a length l on a two-dimensional plane embedded with a set of equidistant parallel lines with a distance d , and studies the statistical properties of intersections between the needle and the lines. Buffon-Laplace Needle Problem [2, 3] is a simple extension of Buffon’s Needle Problem. It considers a similar scenario yet on a plane distributed with two sets of equidistant parallel lines with distances a and b , respectively, which are vertical to each other. For convenience, we set $b \leq a$ in this paper.

The fundamental quantity for the two problems is the intersection probability of a needle intersecting with at least one line. In Buffon’s Needle Problem, for the intersection probability $P(l, d)$ with a needle length l and a line distance d , [1] and [4](page 251-252) show its form for the initial version with $l < d$. [4](page 258, problem 7) also shows $P(l, d)$ for a long needle case with $d < l$. In Buffon-Laplace Needle Problem, for the intersection probability $P(l, a, b)$ with a needle length l and line distances a and b , [2, 3] and [4](page 255-257) show a prediction of the initial case with $l < b$. In [5], the authors further lay down an analytical form of $P(l, a, b)$ in a specific case of $a = b$ with $b < l$ (as Eq. 6 in its main text), yet with an error in a coefficient which we will show later. Another quantity pertinent to the two needle-dropping problems is the distribution of intersections, especially in the case of a long needle. For Buffon’s Needle Problem, [6] shows the distribution of intersections in the case of a needle with $d < l$.

As classical models of randomness, variants based on Buffon’s and Buffon-Laplace Needle Problems are frequently discussed in both mathematical and physical literature. A direct variation of the problems is to generalize needles and lines into other geometrical objects. For Buffon’s Needle Problem, a needle can be substituted with a planar curve [7, 8], polygons [9], a pivot needle (two needles sharing a tip) [10], and so on. Besides, sets

of parallel lines can also be generalized to parallel stripes with a finite width [11], random Cantor sets [12, 13], a line with randomly distributed dots [14], and so on. For Buffon-Laplace Needle Problem, a needle can be replaced by an ellipse [15], a spherocylinder (a cylinder with hemispherical caps on both ends) in three-dimensional space [5], and so on. Besides, a plane in the problem can be considered as being covered with repeated congruent triangles [4] (page 258, problem 8).

Here we revisit Buffon-Laplace Needle Problem and focus on the analytical prediction of intersection probability $P(l, a, b)$, which is simply the fundamental quantity of the problem. The initial case of the problem with $l < b$ is heavily discussed in previous literature, while analytical results in the case of $b < l$ are quite limited, as far as we know. Here we tackle the problem in a general case of any l , especially $b < l$. We have two motivations for this. The first one is mathematical, in which forcing $l < b$ is not necessary for a theoretical model and choosing any l under $b < l$ is still valid in a model definition. The second one is rather physical, as extending to any l represents a more realistic scenario with wider ranges of model parameters when the problem serves as an approximation model in a physical context. For example, in [5] Buffon-Laplace Needle Problem is adopted as a model for granular particles filtering through a sieve-like grid in which a needle is generalized to a rod-like object with finite volume, and setting $l > b$ makes possible studying new complex phenomena originated from long particles.

In this paper, we present a single analytical framework for Buffon-Laplace Needle Problem to calculate the intersection probability $P(l, a, b)$ with any l for given a and b , including the initial version with $l < b$. See Eq.(28) for a concise summary of $P(l, a, b)$, which is our main contribution here.

Here is a layout of the paper. In Section II, we present Buffon-Laplace Needle Problem and a representation of needle position in a grid. In Section III, we explain our analytical framework to calculate the intersection probability $P(l, a, b)$ for any l . In Section IV, we verify our theoretical prediction with numerical simulation. In Section V, we conclude the paper with some discussion.

* zhaojh@m.scnu.edu.cn

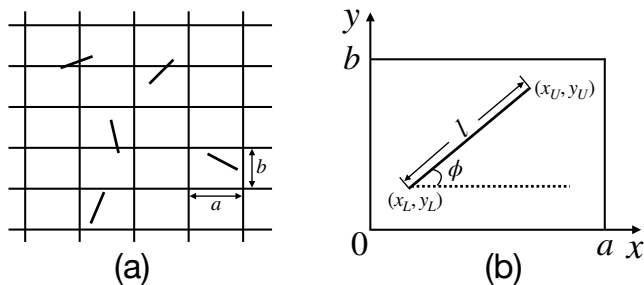


FIG. 1. Setting of Buffon-Laplace Needle Problem. (a) The two sets of vertically parallel lines have distances of a and b , respectively, which form a rectangular grid. The five line segments scattered in the grid represent needles, three of which intersect with the grid. (b) Relative positions of a needle in a grid cell with width a and height b . The coordinates (x_U, y_U) and (x_L, y_L) represent respectively the upper and the lower tips of the needle, and the orientation ϕ is the angle between the needle and the x -axis.

II. MODEL

Fig.1(a) shows a schematic diagram of needles and a rectangular grid for Buffon-Laplace Needle Problem. As being stated, we set $b \leq a$ for line spacings for convenience.

To estimate the intersection probability, it is only relevant to consider whether or not a needle intersects with lines, which only involves the relative position between them. Thus a needle dropping on a large grid can be simplified into a picture in which a needle dropping on a single grid cell with width a and height b . We choose parallel lines with distances b and a to establish x - and y -axis, respectively. A simple description of the relative position of a needle in a grid cell consists of three ingredients: the coordinate x_U on x -axis and the coordinate y_U on y -axis for the upper tip of the needle, and the orientation ϕ between the needle and the x -axis. Their ranges are $[0, a)$, $[0, b)$, and $[0, \pi)$, respectively. Fig.1(b) shows an example.

With the above position representation, we can carry out numerical simulation for the problem. With given parameters (l, a, b) , we generate a large number N_{all} of experiments of tossing needles, count the number N_{coll} of those experiments in which a needle overlaps with at least one boundary of a grid cell, and calculate the intersection probability $P(l, a, b) = N_{\text{coll}}/N_{\text{all}}$. In the Monte Carlo simulation[16] of the problem, we adopt a pseudo-random number generator, say $\text{Rand}()$, which generates a sequence of numbers $\in (0, 1)$ obeying a uniform distribution. In a single experiment, we generate a random configuration of a needle position as

$$\begin{pmatrix} x_U \\ y_U \\ \phi \end{pmatrix} = \begin{pmatrix} a \times \text{Rand}() \\ b \times \text{Rand}() \\ \pi \times \text{Rand}() \end{pmatrix}. \quad (1)$$

Correspondingly, the coordinates of the lower tip of the

needle are

$$\begin{pmatrix} x_L \\ y_L \end{pmatrix} = \begin{pmatrix} x_U - l \cos \phi \\ y_U - l \sin \phi \end{pmatrix}. \quad (2)$$

An intersection between the needle and the grid happens when the condition

$$x_L < 0 \vee a < x_L \vee y_L < 0 \vee b < y_L \quad (3)$$

holds. Beware that, in the numerical simulation with continuous real numbers, we ignore the cases when the two needle tips exactly fall on any boundary of the grid cell (say, $x = 0, a$, and $y = 0, b$), since their probability is infinitesimal.

III. THEORY

Based on the representation of the relative position of a needle in a grid cell in the Model section, we develop an analytical framework to calculate the intersection probability $P(l, a, b)$ with any given l, a, b , which corresponds to the result from an infinitely large number of experiments of needle dropping.

We consider the parameters (x_U, y_U, ϕ) for a needle position in all their ranges, and calculate the part of their ranges when the corresponding (x_L, y_L) leads to an intersection between the needle and the grid. $P(l, a, b)$ can be formulated as

$$P(l, a, b) = \frac{S_{\text{coll}}}{S_{\text{all}}}, \quad (4)$$

in which S_{all} is the volume of whole ranges of (x_U, y_U, ϕ) , and S_{coll} the volume of proper ranges of (x_U, y_U, ϕ) when an intersection is possible. It is easy to find that

$$S_{\text{all}} = (a - 0) \cdot (b - 0) \cdot (\pi - 0) = ab\pi. \quad (5)$$

The challenging part here is to derive an explicit form of S_{coll} . S_{coll} can be derived as

$$S_{\text{coll}} = S_{\text{coll}}(x) + S_{\text{coll}}(y) - S_{\text{coll}}(x, y), \quad (6)$$

in which $S_{\text{coll}}(x)$ denotes the volume of the ranges of (x_U, y_U, ϕ) when an intersection happens on the boundaries of x -axis of a grid cell (say, $x = 0$ and a), $S_{\text{coll}}(y)$ the volume of the ranges of (x_U, y_U, ϕ) when an intersection happens on the boundaries of y -axis of a grid cell (say, $y = 0$ and b), and $S_{\text{coll}}(x, y)$ the volume of the ranges of (x_U, y_U, ϕ) when an intersection happens on the boundaries of x - and y -axes of a grid cell at the same time. The

three terms can be calculated as:

$$\begin{aligned}
S_{\text{coll}}(x) &= \int_0^\pi d\phi \int_0^a \Theta(|l \cos \phi| - x) dx \int_0^b dy \\
&= \int_0^{\frac{\pi}{2}} d\phi \int_0^a \Theta(l \cos \phi - x) dx \int_0^b dy \\
&+ \int_{\frac{\pi}{2}}^\pi d\phi \int_0^a \Theta(-l \cos \phi - x) dx \int_0^b dy, \tag{7}
\end{aligned}$$

$$\begin{aligned}
S_{\text{coll}}(y) &= \int_0^\pi d\phi \int_0^a dx \int_0^b \Theta(l \sin \phi - y) dy, \tag{8}
\end{aligned}$$

$$\begin{aligned}
S_{\text{coll}}(x, y) &= \int_0^\pi d\phi \int_0^a \Theta(|l \cos \phi| - x) dx \int_0^b \Theta(l \sin \phi - y) dy \\
&= \int_0^{\frac{\pi}{2}} d\phi \int_0^a \Theta(l \cos \phi - x) dx \int_0^b \Theta(l \sin \phi - y) dy \\
&+ \int_{\frac{\pi}{2}}^\pi d\phi \int_0^a \Theta(-l \cos \phi - x) dx \int_0^b \Theta(l \sin \phi - y) dy
\end{aligned}$$

In the above multiple integrals, the step function $\Theta(x)$ is defined as $\Theta(x) = 1$ if $x \geq 0$ and 0 otherwise. Combining a step function into integrations on the three parameters (x_U, y_U, ϕ) singles out their proper ranges which permit an intersection between a needle and a grid cell. In the second equal signs of Eqs.(7) and (9), we split $\int_0^\pi d\phi[\cdot]$ into $\int_0^{\frac{\pi}{2}} d\phi[\cdot]$ and $\int_{\frac{\pi}{2}}^\pi d\phi[\cdot]$.

To finish the computation of integrals in Eqs.(7) - (9), we should examine the relative sizes of l , a , and b , which are shown schematically in Fig.2. We will detail four cases below.

A. The case of $l \leq b$

We first consider the case of $l \leq b$. See Fig.2 (a) and (c) for an illustration. This case corresponds to the initial version of Buffon-Laplace Needle Problem[2, 3].

Here we simply have $|l \cos \phi| \leq a$ and $l \sin \phi \leq b$ for any $\phi \in [0, \pi)$. For $S_{\text{coll}}(x)$, with Eq.(7) we have

$$\begin{aligned}
S_{\text{coll}}(x) &= \int_0^{\frac{\pi}{2}} d\phi \int_0^{l \cos \phi} dx \cdot b + \int_{\frac{\pi}{2}}^\pi d\phi \int_0^{-l \cos \phi} dx \cdot b \\
&= 2bl. \tag{10}
\end{aligned}$$

For $S_{\text{coll}}(y)$, with Eq.(8) we have

$$\begin{aligned}
S_{\text{coll}}(y) &= \int_0^\pi d\phi \cdot a \cdot \int_0^{l \sin \phi} dy \\
&= 2al. \tag{11}
\end{aligned}$$

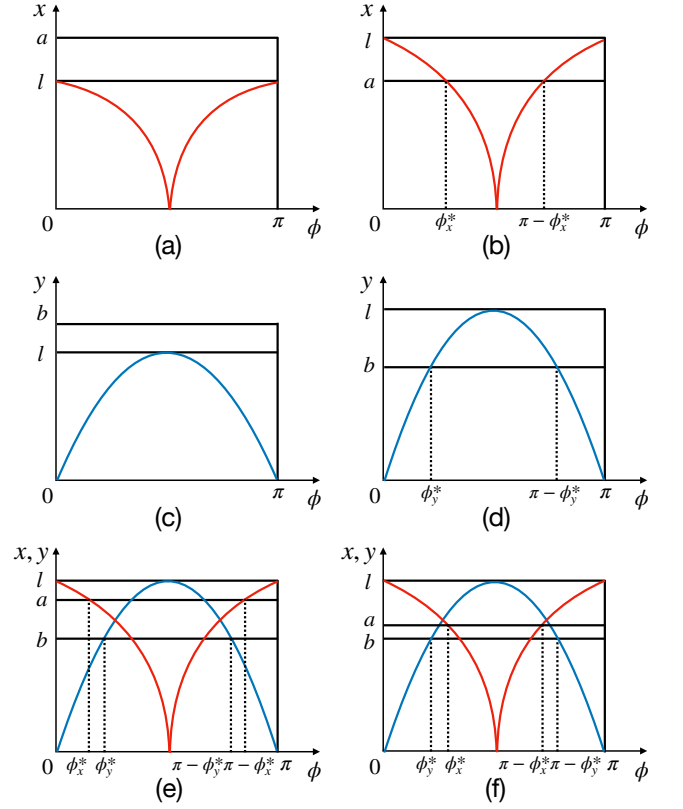


FIG. 2. Cases of relative sizes of l , a , and b . (a) shows the curve $x = |l \cos \phi|$ under the condition $l \leq a$. (b) shows the same as (a), yet with $a < l$. $\phi_x^* \in (0, \pi/2)$ and $\pi - \phi_x^*$ are the ϕ -coordinates of the two points where the lines $x = a$ and $x = |l \cos \phi|$ intersect. (c) shows the curve $y = l \sin \phi$ under the condition $l \leq b$. (d) shows the same as (c), yet with $b < l$. $\phi_y^* \in (0, \pi/2)$ and $\pi - \phi_y^*$ are the ϕ -coordinates of the two points where the lines $y = b$ and $y = l \sin \phi$ intersect. (e) shows the curve $x = |l \cos \phi|$ and $y = l \sin \phi$ at the same time under the condition $\phi_x^* \leq \phi_y^*$ or equivalently $l \leq \sqrt{a^2 + b^2}$. (f) shows the same as (e), yet with $\phi_y^* < \phi_x^*$ or equivalently $\sqrt{a^2 + b^2} < l$.

For $S_{\text{coll}}(x, y)$, with Eq.(9) we have

$$\begin{aligned}
S_{\text{coll}}(x, y) &= \int_0^{\frac{\pi}{2}} d\phi \int_0^{l \cos \phi} dx \int_0^{l \sin \phi} dy \\
&+ \int_{\frac{\pi}{2}}^\pi d\phi \int_0^{-l \cos \phi} dx \int_0^{l \sin \phi} dy \\
&= l^2. \tag{12}
\end{aligned}$$

Thus, with Eq.(6) we have

$$S_{\text{coll}} = 2bl + 2al - l^2. \tag{13}$$

Finally, with Eq.(4) we have

$$P(l, a, b) = \frac{2}{\pi} \left(\frac{l}{a} + \frac{l}{b} \right) - \frac{1}{\pi} \frac{l^2}{ab}. \tag{14}$$

B. The case of $b < l \leq a$

Here we have $|l \cos \phi| \leq a$ for any $\phi \in [0, \pi)$, yet $l \sin \phi \leq b$ holds for ϕ in some partial range of $[0, \pi)$. We define $l \sin \phi_y^* = b$ while $\phi_y^* \in (0, \pi/2)$, thus $\phi_y^* = \arcsin \frac{b}{l}$. See Fig.2 (a) and (d) for an illustration.

For $S_{\text{coll}}(x)$, we have

$$\begin{aligned} S_{\text{coll}}(x) &= \int_0^{\frac{\pi}{2}} d\phi \int_0^{l \cos \phi} dx \cdot b + \int_{\frac{\pi}{2}}^{\pi} d\phi \int_0^{-l \cos \phi} dx \cdot b \\ &= 2bl. \end{aligned} \quad (15)$$

For $S_{\text{coll}}(y)$, we have

$$\begin{aligned} S_{\text{coll}}(y) &= \int_0^{\phi_y^*} d\phi \cdot a \cdot \int_0^{l \sin \phi} dy + \int_{\phi_y^*}^{\pi - \phi_y^*} d\phi \cdot a \cdot \int_0^b dy \\ &+ \int_{\pi - \phi_y^*}^{\pi} d\phi \cdot a \cdot \int_0^{l \sin \phi} dy \\ &= 2al(1 - \cos \phi_y^*) + ab(\pi - 2\phi_y^*) \\ &= 2al \left[1 - \sqrt{1 - \left(\frac{b}{l}\right)^2} \right] + ab \left(\pi - 2 \arcsin \frac{b}{l} \right) \end{aligned} \quad (16)$$

For $S_{\text{coll}}(x, y)$, we have

$$\begin{aligned} S_{\text{coll}}(x, y) &= \int_0^{\phi_y^*} d\phi \int_0^{l \cos \phi} dx \int_0^{l \sin \phi} dy \\ &+ \int_{\phi_y^*}^{\frac{\pi}{2}} d\phi \int_0^{l \cos \phi} dx \int_0^b dy \\ &+ \int_{\frac{\pi}{2}}^{\pi - \phi_y^*} d\phi \int_0^{-l \cos \phi} dx \int_0^b dy \\ &+ \int_{\pi - \phi_y^*}^{\pi} d\phi \int_0^{-l \cos \phi} dx \int_0^{l \sin \phi} dy \\ &= l^2 \sin^2 \phi_y^* + 2bl(1 - \sin \phi_y^*) \\ &= 2bl - b^2. \end{aligned} \quad (17)$$

Then, we have

$$\begin{aligned} S_{\text{coll}} &= b^2 + 2al \left[1 - \sqrt{1 - \left(\frac{b}{l}\right)^2} \right] \\ &+ ab \left(\pi - 2 \arcsin \frac{b}{l} \right). \end{aligned} \quad (18)$$

Finally, we have

$$\begin{aligned} P(l, a, b) &= \frac{1}{\pi} \frac{b}{a} + \frac{2}{\pi} \frac{l}{b} \left[1 - \sqrt{1 - \left(\frac{b}{l}\right)^2} \right] \\ &+ \left(1 - \frac{2}{\pi} \arcsin \frac{b}{l} \right). \end{aligned} \quad (19)$$

C. The cases in $a < l$

Here both $|l \cos \phi| \leq a$ and $l \sin \phi \leq b$ hold for ϕ in some partial range of $[0, \pi)$. We define $l \cos \phi_x^* = a$ while $\phi_x^* \in (0, \pi/2)$, thus $\phi_x^* = \arccos \frac{a}{l}$. We also define $l \sin \phi_y^* = b$ while $\phi_y^* \in (0, \pi/2)$, thus $\phi_y^* = \arcsin \frac{b}{l}$. See Fig.2 (b) and (d) for an illustration.

For $S_{\text{coll}}(x)$, we have

$$\begin{aligned} S_{\text{coll}}(x) &= \int_0^{\phi_x^*} d\phi \int_0^a dx \cdot b + \int_{\phi_x^*}^{\frac{\pi}{2}} d\phi \int_0^{l \cos \phi} dx \cdot b \\ &+ \int_{\frac{\pi}{2}}^{\pi - \phi_x^*} d\phi \int_0^{-l \cos \phi} dx \cdot b + \int_{\pi - \phi_x^*}^{\pi} d\phi \int_0^a dx \cdot b \\ &= 2bl(1 - \sin \phi_x^*) + 2ab\phi_x^* \\ &= 2bl \left[1 - \sqrt{1 - \left(\frac{a}{l}\right)^2} \right] + 2ab \arccos \frac{a}{l}. \end{aligned} \quad (20)$$

For $S_{\text{coll}}(y)$, we have

$$\begin{aligned} S_{\text{coll}}(y) &= \int_0^{\phi_y^*} d\phi \cdot a \cdot \int_0^{l \sin \phi} dy + \int_{\phi_y^*}^{\pi - \phi_y^*} d\phi \cdot a \cdot \int_0^b dy \\ &+ \int_{\pi - \phi_y^*}^{\pi} d\phi \cdot a \cdot \int_0^{l \sin \phi} dy \\ &= 2al(1 - \cos \phi_y^*) + ab(\pi - 2\phi_y^*) \\ &= 2al \left[1 - \sqrt{1 - \left(\frac{b}{l}\right)^2} \right] + ab \left(\pi - 2 \arcsin \frac{b}{l} \right) \end{aligned} \quad (21)$$

To further calculate $S_{\text{coll}}(x, y)$ we should check the relative size of ϕ_x^* and ϕ_y^* , whose different choices lead to different integrands in the integrals of $S_{\text{coll}}(x, y)$. When $\phi_x^* \leq \phi_y^*$, we correspondingly have $\sin^2 \phi_x^* \leq \sin^2 \phi_y^*$. Equivalently, $1 - a^2/l^2 \leq b^2/l^2$, or $l \leq \sqrt{a^2 + b^2}$. When $\phi_y^* < \phi_x^*$, we easily have $\sqrt{a^2 + b^2} < l$. See Fig.2 (e) and (f) for an illustration. Calculation of $S_{\text{coll}}(x, y)$ in the two cases are listed below.

When $a < l \leq \sqrt{a^2 + b^2}$, equivalently $\phi_x^* \leq \phi_y^*$, we have

$$\begin{aligned} S_{\text{coll}}(x, y) &= \int_0^{\phi_x^*} d\phi \int_0^a dx \int_0^{l \sin \phi} dy \\ &+ \int_{\phi_x^*}^{\phi_y^*} d\phi \int_0^{l \cos \phi} dx \int_0^{l \sin \phi} dy \\ &+ \int_{\phi_y^*}^{\frac{\pi}{2}} d\phi \int_0^{l \cos \phi} dx \int_0^b dy \\ &+ \int_{\frac{\pi}{2}}^{\pi - \phi_y^*} d\phi \int_0^{-l \cos \phi} dx \int_0^b dy \\ &+ \int_{\pi - \phi_y^*}^{\pi} d\phi \int_0^{-l \cos \phi} dx \int_0^{l \sin \phi} dy \end{aligned}$$

$$\begin{aligned}
& + \int_{\pi-\phi_x^*}^{\pi} d\phi \int_0^a dx \int_0^{l \sin \phi} dy \\
& = 2al(1 - \cos \phi_x^*) + 2bl(1 - \sin \phi_y^*) \\
& + l^2 (\cos^2 \phi_x^* + \sin^2 \phi_y^* - 1) \\
& = 2al - a^2 + 2bl - b^2 - l^2. \tag{22}
\end{aligned}$$

Thus, we have

$$\begin{aligned}
S_{\text{coll}} & = a^2 + b^2 + l^2 - 2 \left(b\sqrt{l^2 - a^2} + a\sqrt{l^2 - b^2} \right) \\
& + ab \left(\pi - 2 \arcsin \frac{b}{l} + 2 \arccos \frac{a}{l} \right). \tag{23}
\end{aligned}$$

Correspondingly, we have

$$\begin{aligned}
P(l, a, b) & = \frac{1}{\pi} \left(\frac{a}{b} + \frac{b}{a} + \frac{l^2}{ab} \right) \\
& - \frac{2}{\pi} \left[\sqrt{\left(\frac{l}{a}\right)^2 - 1} + \sqrt{\left(\frac{l}{b}\right)^2 - 1} \right] \\
& + \left(1 - \frac{2}{\pi} \arcsin \frac{b}{l} + \frac{2}{\pi} \arccos \frac{a}{l} \right). \tag{24}
\end{aligned}$$

When $\sqrt{a^2 + b^2} < l$, equivalently $\phi_y^* < \phi_x^*$, we have

$$\begin{aligned}
S_{\text{coll}}(x, y) & = \int_0^{\phi_y^*} d\phi \int_0^a dx \int_0^{l \sin \phi} dy + \int_{\phi_y^*}^{\phi_x^*} d\phi \int_0^a dx \int_0^b dy \\
& + \int_{\phi_x^*}^{\frac{\pi}{2}} d\phi \int_0^{l \cos \phi} dx \int_0^b dy \\
& + \int_{\frac{\pi}{2}}^{\pi-\phi_x^*} d\phi \int_0^{-l \cos \phi} dx \int_0^b dy \\
& + \int_{\pi-\phi_x^*}^{\pi-\phi_y^*} d\phi \int_0^a dx \int_0^b dy + \int_{\pi-\phi_y^*}^{\pi} d\phi \int_0^a dx \int_0^{l \sin \phi} dy \\
& = 2al(1 - \cos \phi_y^*) + 2bl(1 - \sin \phi_x^*) + 2ab(\phi_x^* - \phi_y^*) \\
& = 2al \left[1 - \sqrt{1 - \left(\frac{b}{l}\right)^2} \right] + 2bl \left[1 - \sqrt{1 - \left(\frac{a}{l}\right)^2} \right] \\
& + 2ab \left(\arccos \frac{a}{l} - \arcsin \frac{b}{l} \right). \tag{25}
\end{aligned}$$

Then, we have

$$S_{\text{coll}} = ab\pi, \tag{26}$$

after most terms cancel out. Correspondingly, we have

$$P(l, a, b) = 1. \tag{27}$$

The above result has an intuitive geometrical interpretation. The longest distance between two points in a grid cell with width a and height b is from the diagonal line with a distance of $\sqrt{a^2 + b^2}$. Thus any needle with a length $l > \sqrt{a^2 + b^2}$ dropping on a grid is certain to intersect with the grid boundaries, leading to $P(l, a, b) = 1$.

D. Summing results

Summing the above results of four cases in Eqs. (14), (19), (24), and (27), we have

$$P(l, a, b) = \begin{cases} \frac{2}{\pi} \left(\frac{l}{a} + \frac{l}{b} \right) - \frac{l^2}{\pi ab}, & \text{if } l \leq b; \\ \frac{1}{\pi} \frac{b}{a} + \frac{2}{\pi} \frac{l}{b} \left[1 - \sqrt{1 - \left(\frac{b}{l}\right)^2} \right] \\ + \left(1 - \frac{2}{\pi} \arcsin \frac{b}{l} \right), & \text{if } b < l \leq a; \\ \frac{1}{\pi} \left(\frac{a}{b} + \frac{b}{a} + \frac{l^2}{ab} \right) \\ - \frac{2}{\pi} \left[\sqrt{\left(\frac{l}{a}\right)^2 - 1} + \sqrt{\left(\frac{l}{b}\right)^2 - 1} \right] \\ + \left(1 - \frac{2}{\pi} \arcsin \frac{b}{l} + \frac{2}{\pi} \arccos \frac{a}{l} \right), & \text{if } a < l \leq \sqrt{a^2 + b^2}; \\ 1, & \text{if } \sqrt{a^2 + b^2} < l. \end{cases} \tag{28}$$

The above framework retrieves the result for the initial case of $l < b$ as in [2, 3]. Our main contribution here to Buffon-Laplace Needle Problem is the analytical result in the cases of $b < l \leq a$ and $a < l \leq \sqrt{a^2 + b^2}$.

A necessary condition for the correctness of Eq.(28) is the consistency of $P(l, a, b)$, equivalently S_{coll} , at the boundaries of the four cases of l . When $l = b$, both the calculations in the cases of $l \leq b$ and $b < l \leq a$ reduce to

$$S_{\text{coll}} = b^2 + 2ab. \tag{29}$$

When $l = a$, both the calculations in the cases of $b < l \leq a$ and $a < l \leq \sqrt{a^2 + b^2}$ reduce to

$$\begin{aligned}
S_{\text{coll}} & = 2a^2 + b^2 - 2a\sqrt{a^2 - b^2} + ab \left(\pi - 2 \arcsin \frac{b}{a} \right) \tag{30}
\end{aligned}$$

When $l = \sqrt{a^2 + b^2}$, the calculation in the case of $a < l \leq \sqrt{a^2 + b^2}$ reduces to

$$S_{\text{coll}} = ab\pi, \tag{31}$$

which equals S_{coll} in the case of $\sqrt{a^2 + b^2} < l$.

We further compare our equations with a previous one. The paper [5] considers a special case with $a = b = 1$, and derives the intersection probability for $b < l$ in Eq. (6) in its main text. Based on the expression for $a < l \leq \sqrt{a^2 + b^2}$ in Eq.(28) here and setting $a = b = 1$, after some calculation we have

$$\begin{aligned}
P(l, 1, 1) & = \\
& 1 - \frac{2}{\pi} \left(\arcsin \frac{1}{l} - \arccos \frac{1}{l} + 2\sqrt{l^2 + 1} - \frac{l^2}{2} - 1 \right) \tag{32}
\end{aligned}$$

We can easily find that there is an error in Eq.(6) of [5] as the coefficient $1/\pi$ of the second term should be $2/\pi$ as we show above.

E. Reducing to Buffon's Needle Problem

Setting the distance $a \rightarrow \infty$, the constraint on intersection from the x -axis vanishes, and Buffon-Laplace Needle

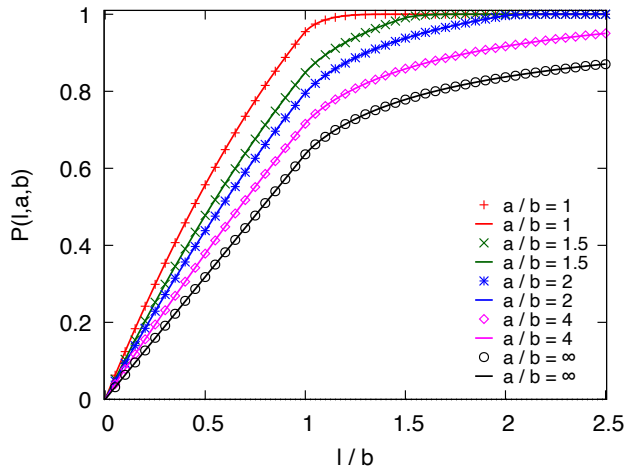


FIG. 3. Result of Buffon-Laplace Needle Problem. We show the intersection probability $P(l, a, b)$ versus the ratio l/b . From above to below, we show results when $a/b = 1, 1.5, 2, 4, \infty$, the last of which corresponds to Buffon's Needle Problem. Signs are results from Monte Carlo simulation with $b = 3.0$ and a needle-dropping size $N_{\text{all}} = 10^6$. Lines are analytical results from Eq.(28).

Problem reduces to Buffon's Needle Problem. On the analytical side, as $l/a \rightarrow 0$, Eqs.(14) and (19) simplify to

$$P(l, \infty, b) = \begin{cases} \frac{2}{\pi} \frac{l}{b}, & \text{if } l \leq b; \\ \frac{2}{\pi} \frac{l}{b} \left[1 - \sqrt{1 - \left(\frac{b}{l}\right)^2} \right] + \left(1 - \frac{2}{\pi} \arcsin \frac{b}{l} \right), & \text{if } b < l, \end{cases} \quad (33)$$

which is just the analytical result of Buffon's Needle Problem [4].

IV. RESULT

To verify our analytical result summed in Eq.(28), we perform Monte Carlo simulation of needle-dropping explained in the Model section, and derive empirical result for $P(l, a, b)$. Fig.3 shows both results from numerical simulation and our analytical theory, which coincide very well.

V. CONCLUSION

We study here Buffon-Laplace Needle Problem on its theoretical solution of intersection probability $P(l, a, b)$ with any l . With a single probabilistic framework, we not only retrieve the result on the initial version with $l < b$, but also derive explicit expressions of $P(l, a, b)$ in the cases of $b < l \leq a$ and $a < l \leq \sqrt{a^2 + b^2}$ which are absent in previous literature as far as we know. We further validate our theoretical prediction with Monte Carlo simulation.

There are already a few variants and extensions of Buffon's and Buffon-Laplace Needle Problems both in their original versions of a 'short' needle with mathematical and physical significance. We hope that our analytical framework here, which applies to any needle length, could inspire principled theoretical approaches to realistic generalizations of these models.

ACKNOWLEDGEMENTS

This work is supported by Guangdong Major Project of Basic and Applied Basic Research No. 2020B0301030008 and Guangdong Basic and Applied Basic Research Foundation (Grant No. 2022A1515011765).

-
- [1] Buffon G-L. Essai d'arithmétique morale. Histoire naturelle, générale et particulière, Supplément 1777; 4: 46-123.
 - [2] Laplace P-S. Théorie analytique des probabilités. Paris: Veuve Courcier; 1812.
 - [3] Laplace P-S. Théorie analytique des probabilités. Third Revised Edition. Paris: Veuve Courcier; 1820.
 - [4] Uspensky J V. Introduction to Mathematical Probability. New York: McGraw-Hill; 1937.
 - [5] Dell Z E and Franklin S V. The Buffon-Laplace needle problem in three dimensions. J Stat Mech 2009; P09010.
 - [6] Diaconis P. Buffon's Problem with a long needle. J Appl Prob 1976; 13: 614-8.
 - [7] Barbier E. Note sur le problème de l'aiguille et le jeu du joint couvert. J Math Pur App 1860; 5: 273-86.
 - [8] Ramaley J F. Buffon's Noodle Problem. Am Math Mon 1969; 76: 916-8.
 - [9] Johannesen I G. The Buffon needle problem revisited in a pedagogical perspective. Math J 2009; 11: 284-99.
 - [10] Basel U. Buffon's problem with a pivot needle. Elem Math 2015; 70: 67-70.
 - [11] Chung C F. Application of the Buffon Needle Problem and its extensions to parallel-line search sampling scheme. Math Geo 1981; 12: 371-90.
 - [12] Zhang S. The exact power law for Buffon's needle landing near some random Cantor sets. Rev Mat Iberoam 2020; 36: 537-48.
 - [13] Vardakis D and Volberg A. The Buffon's needle problem for random planar disk-like Cantor sets. J Math Anal Appl 2024; 529: 127622.
 - [14] Godrèche C. The Buffon needle problem for Lévy distributed spacings and renewal theory. J Stat Mech 2022; 013203.
 - [15] Duma A and Stoka M. Hitting probabilities for random ellipses and ellipsoids. J Appl Prob 1993; 30: 971-4.
 - [16] Landau D P and Binder K. A Guide to Monte Carlo Simulations in Statistical Physics. Fourth Edition. Cambridge: Cambridge University Press; 2015.